
FEATURE SELECTION INTEGRATED DEEP LEARNING FOR ULTRAHIGH DIMENSIONAL AND HIGHLY CORRELATED FEATURE SPACE

Arkaprabha Ganguli, Tapabrata Maiti

Department of Statistics and Probability
Michigan State University
`{gangulia, maiti}@msu.edu`

ABSTRACT

In recent years, deep learning has been a topic of interest in almost all disciplines due to its impressive empirical success in analyzing complex data sets, such as imaging, genetics, climate, and medical data. While most of the developments are treated as black-box machines, there is an increasing interest in interpretable, reliable, and robust deep learning models applicable to a broad class of applications. Feature-selected deep learning is proven to be promising in this regard. However, the recent developments do not address the situations of ultra-high dimensional and highly correlated feature selection in addition to the high noise level. In this article, we propose a novel screening and cleaning strategy with the aid of deep learning for the cluster-level discovery of highly correlated predictors with a controlled error rate. A thorough empirical evaluation over a wide range of simulated scenarios demonstrates the effectiveness of the proposed method by achieving high power while having a minimal number of false discoveries. Furthermore, we implemented the algorithm in the riboflavin (vitamin B_2) production dataset in the context of understanding the possible genetic association with riboflavin production. The gain of the proposed methodology is illustrated by achieving lower prediction error compared to other state-of-the-art methods.

Keywords Nonlinear Feature selection · Deep Neural Network · False discovery Rate · LassoNet · High-dimensional data · Multicollinearity · Resampling · error-controoled

1 Introduction

For the past few decades, the feature screening problem is of particular interest as streams of large data sets are arising from a wide range of application domains covering from astrophysics to genetics, from finance industry to epidemiological studies and many more. As nicely discussed in [3], the main objective of a feature selection method is to find the best subset of features in order to attain a deeper knowledge on the relationship between the features and the response aiding in further scientific investigation. This offers improved interpretability and explainability, reduced computational cost for prediction and estimation, and less memory usage by estimating a lower dimensional manifold of the feature space. However, approximating the true data generating process is often a daunting task in practice, especially when the sample size is much smaller than the dimension of the feature space. Under linear model framework, this problem has been extensively studied over the past few decades and we have several algorithms such as Lasso, Elastic net, SCAD, MCP and many more; a detailed review can be found at Fan and Lv [10] and thus omitted here.

Relaxing the linear assumption, the Artificial Neural Network (ANN) models are well known for efficiently approximating complicated functions. From information-theoretic viewpoint, [9] established that the deep neural networks provide optimal approximation of a nonlinear function covering a wide range of functional classes used in signal processing. This fosters the use of Deep Learning (DL) models for feature selection which has become a major research interest over past few years. On the other hand, the DL models are well known for their black box nature. Following the intriguing

arguments in [25], caution must be exercised regarding the application of DL models for decision making in real world problems throughout society. Employing only the relevant predictors to construct a predictive model is obviously a right step towards the explainable machine learning. However, as suggested in [12], often the feature importance in DL-based algorithms varied drastically under small perturbation in the input or in the presence of added noise. This casts serious doubts on the variable selection algorithms and to mitigate this, guaranteeing some sort of replicability is of immense importance. That implies, controlling excessive number of false discoveries aids in bringing back the reliability and explainability into the DL-based feature selection methods.

As a solution to this problem, we focus on reproducible nonlinear variable selection using DL models with some sort of error control. In this work, we choose to control the False Discovery Rate (FDR) first proposed by [2] as it is more suited to large-scale multiple testing problems. To formally define the FDR, we consider the following random variable FDP representing the False Discovery Proportion: $FDP = \frac{e_0}{N_+} \mathbf{1} (N_+ > 0)$, where e_0 = number of falsely selected variables and N_+ = number of total discoveries. Then, FDR is defined as $FDR = E(FDP)$. Estimating this expectation poses an unique challenge for the model-free variable selection problem and many authors have tried to solve this from various perspectives. Extensive research has been done using p-values as feature importance in multiple testing context; see [31, 34, 19, 17] for more detailed overview. However, for DL models, generating interpretable p-values is still an unrevealed research problem. To avoid this, the knockoff framework has been proposed by [7] entertaining a model free variable selection algorithm with provable FDR control, assuming prior knowledge is available about the predictor distribution. [22] proposed the *DeepPINK* algorithm integrating the knockoff framework with the DL architecture for improved explainability of the DL models. However in real world applications, the predictors' distribution has to be estimated to generate the knockoff variables, and recently [1] showed that the knockoff framework suffers from yielding an inflation in false discoveries in accordance with the error incurred in estimating the predictor's distribution; see section for an empirical evidence. In some cases, there are available prior knowledge on the correlation pattern among the features; like in the genetics studies, where there is a common notion of linkage disequilibrium indicating the dependence pattern between the alleles at polymorphisms ([26]). However, in other application domain, this might not be available. Hence any model-specific knockoff generation would be inefficient in those contexts. Recently, DL-based flexible knockoff generating algorithms have been proposed [21, 15, 24]; however they are trained in a typical big- n -small- p setting and it is unclear how they will perform when the sample size n is significantly smaller than the dimension of the covariates p , and the predictors are highly correlated. We next discuss the multicollinearity issue.

In most of the modern high-dimensional datasets arising in genetics and imaging studies, the other challenge is extreme multicollinearity - the predictors are typically correlated among themselves in a complex manner; often with the sample correlations greater than 0.99, or even equalling to 1. This setting is typically known to be problematic for traditional variable selection problems. An empirical illustration is provided in the section 3 of the supplementary material showing how model-X knockoff method [7] typically fails to control FDR under a simplistic setting with high multicollinearity. As the extremely correlated variables become almost indistinguishable, in regression setup, it would be unfeasible to claim specifically that one of them is associated with the outcome. Accounting for the uncertainty, it would be pragmatic to aim for group level variable selection and claim that at least one variable from a densely correlated group is important for the outcome. Accordingly, the term '*true discovery*' implies that the selected cluster can serve as a good proxy for at least one element in the true index set S_0 . As a consequence, the definition of FDR becomes non-trivial and here we adopt the cluster version of the FDR that implies *expected value of the "proportion of clusters that are falsely declared among all declared clusters"*, following [29]. For the rest of the paper, we call this as *cFDR*. [7] also adopted this heuristic approach for their application where the predictors are clustered according to there correlation. However, they typically considered the marginal correlation between two predictors for the cluster formation resulting inflation in cluster size. The precision matrix is generally sparser than usual covariance matrix; so the use of conditional correlation for cluster formation can produce much smaller, yet more interpretable clusters compared to marginal correlation. We adopt this notion in our algorithm which is illustrated in detail in the following sections. Looking at the extreme multicollinearity problem from a slightly different angle, several algorithms have been proposed in the hierarchical testing literature including *CAVIAR* [14], *SUSIE* [33], *KnockoffZoom* [27]. While the knockoff-based procedures have the limitation of generating knockoffs from an unknown distribution with very small sample size, other methods lack in their applicability in non-linear-nonparametric setup as they typically depend on p-values.

Our contribution To mitigate the above mentioned complexity in variable selection and unexplored gap while applying DL, we propose SciDNet- Screening & Cleaning Incorporated Deep Neural Network - a novel method for the reproducible high-dimensional nonlinear-nonparametric feature selection with highly correlated predictors. In order to overcome the challenges related to high-dimension-low-sample-size data, we effectively utilize resampling techniques resulting in both accurate feature selection and reduced prediction error. To fix the ideas, we define the unknown true index set of important predictors as $S_0 \subset \{1, 2, \dots, p\}$ that harbor the variability which influences the response y . Because of strong multicollinearity, some elements of S_0 might be hindered by their highly correlated

proxy counterparts and it would not be feasible to uncover S_0 in individual variable resolution. To alleviate this problem, we divide our method in two parts: **Screening** and **Cleaning**. The screening step is a dimension reduction step. We screen out most of the null variables and select an active set of variables \hat{S}_n which will contain all the proxy variables needed to cover the true set S_0 with high probability. To reduce the high amount of correlation in the active set, by exploiting their conditional dependency structure, we divide the active variables $\{X_j : j \in \hat{S}_n\}$ into $p_c (< p)$ non-overlapping clusters: C_1, C_2, \dots, C_{p_c} and select an appropriate representative from each of the clusters. By sure screening property, with asymptotically high probability, $S_0 \subset \bigcup_{j=1}^{p_c} C_j$. In cleaning step, using a properly tuned DL model under an appropriate resampling scheme, an estimator of the falsely discovered clusters has been proposed followed by developing a surrogate of the FDR. Finally by controlling the surrogate FDR, we select some clusters of highly correlated predictors. To this end, 'FDR observed for SciDNet' would implicitly mean the value of the cFDR discussed here.

To the best of our knowledge, in high-dimensional setting, there is no other method in the literature managing the multicollinearity issue via data adaptive cluster formation followed by the nonlinear-nonparametric controlled feature selection integrated in DL. Our thorough empirical study demonstrates the proposed method's validity in general as a proof of concept by achieving higher power, controlled FDR and higher prediction accuracy. The proposed approach doesn't rely on any modelling assumptions and completely independent of p-value unlike the other state-of-the-art methods, aiding the better understanding of the sparse relationship between the outcome and the high-dimensional predictors. While theoretically guaranteed FDR control in DL-framework is still under active research and lacks a rigorous mathematical foundation, the current study further opens up theoretical investigation for generalizability and broader validity which would be our follow up project.

For the rest of the article, in section 2, we describe the proposed screening and cleaning method, followed by an extensive simulation study in section 3 and application on the riboflavin production dataset in section 4. And finally we conclude at section 5 with a summary and future directions.

2 The Algorithm

Under supervised learning framework, let Y denote a continuous response variable, and $X = (X_1, \dots, X_p)$ denote p continuous covariates. Let n denote the sample size. Here we entertain the ultrahigh-dimensional setting, where $p = O(\exp(n^\tau))$, $\tau > 0$. Maintaining the sparsity condition, we may assume that there exists a subset $S_0 \subset \{1, 2, \dots, p\}$ such that, conditional on features in S_0 , the response Y is independent of features in the complement S_0^c . In other words, $S_0 = \{k : f(y|X) \text{ depends on } X_k\}$, where $f(y|X)$ is the conditional density of y given X . Our goal is to learn the sparsity structure by estimating S_0 .

2.1 Screening Step

Under the assumption that dimensionality of S_0 is much smaller than n , most of the features belong to S_0^c . The screening step is divided in two parts. First, we will screen out most of the null predictors using a model free feature screening algorithm and retain the remaining active set of variables \hat{S}_n . As these active variables are highly correlated among themselves, in second step we further cluster them by exploiting the conditional dependency structure.

2.1.1 Finding the active set of variables

Following the work proposed by [20], [13], [35], for finding the active set, we first consider the non-paranormal transformation on (Y, X) and then perform the Henze–Zirkler's (HZ) test on the transformed variable. While the first transforms all the variables to a joint Gaussian variable maintaining their conditional covariance structure; the second test confirms, by pairwise testing, if there are significant dependence in the transformed response and predictors. We proceed as follows:

1. Let $F_y(\cdot)$ denote the CDF of the response variable Y , and let $F_k(\cdot)$ denote the CDF of the predictor X_k . We consider the nonparanormal transformation as follows: $T_y(Y) = \Phi^{-1}(F_y(Y))$, $T_k(X_k) = \Phi^{-1}(F_k(X_k))$, $k = 1, 2, \dots, p$, where $\Phi(\cdot)$ denotes the CDF of the standard Gaussian distribution. By [20], $(T_y(Y), T_k(X_k))$ will jointly follow a bivariate Gaussian distribution $N_2(0, I_2)$ if $X_k \in S_0^c$ and this can be tested using Henze–Zirkler's test, [13]. For $X_k \in S_0$, the Henze–Zirkler's test statistic is expected to be typically high indicating significant evidence against the independence of the transformed variable $(T_y(Y), T_k(X_k))$.

In practice, the cdf of Y and X_k are unknown, we can estimate it by the truncated empirical cdf as suggested by [20], which is theoretically guaranteed under mild assumptions on nonparanormal distribution. Henceforth, let $(\tilde{T}_y(Y), \tilde{T}_k(X_k))$ denote the corresponding transformations.

2. Next for each predictor X_k , we calculate the the Henze–Zirkler test statistic

$$\tilde{w}_k^* = \frac{1}{n^2} \sum_{i=1}^n \sum_{j=1}^n e^{-\frac{\beta^2}{2} d_{ij}} - \frac{2}{n(1+\beta^2)} \sum_{i=1}^n e^{-\frac{\beta^2}{2(1+\beta^2)} d_i} + \frac{1}{1+2\beta^2} \quad (1)$$

where $d_{ij} = (\tilde{T}_k(x_{ki}) - \tilde{T}_k(x_{kj}))^2 + (\tilde{T}_Y(y_i) - \tilde{T}_Y(y_j))^2$ and $d_i = \tilde{T}_k^2(x_{ki}) + \tilde{T}_Y^2(y_i)$. Consistent with the existing literature, we choose the value of the smoothing parameter β as $\frac{(1.25n)^{1/6}}{\sqrt{2}}$, which corresponds to the optimal bandwidth for a nonparametric kernel density estimator with Gaussian kernel ([13]). The test statistics \tilde{w}_k^* typically represents the averaged difference between the characteristic function of the transformed variable and the characteristic function of $N(0, I_2)$.

3. Next, we select the active set of predictors \hat{S}_n according to the larger values of \tilde{w}_k^* , i.e.,

$$\hat{S}_n = \{1 \leq k \leq p : \tilde{w}_k^* > cn^{-\kappa}\} \quad (2)$$

where where c and κ are predetermined threshold values.

This active set \hat{S}_n contains all the predictors significantly correlated with the response marginally. Under very mild regularity conditions which are generally required for ultrahigh dimensional feature selection, the screening process enjoys the advantage of sure screening property, i.e., $P(S_0 \subset \hat{S}_n) \rightarrow 1$, as $n \rightarrow \infty$. More details on the theoretical guarantee can be found at [35]. Common practice is to set active set size $|\hat{S}_n|$ at $\nu_n = [n/\log(n)]$. However as we further cluster the active variables in the next step, our proposed method is fairly robust in terms of the $|\hat{S}_n|$ as long as we retain most of the significant variables and hence we propose to select a bigger active set with size proportional to ν_n .

2.1.2 Clustering the active predictors using precision matrix

As the Henze–Zirkler test focuses on (pairwise) marginal correlation among the predictors and response, it typically includes all those null predictors having strong association with a significant predictor; and thus they are highly correlated among themselves. The use of sparse precision matrix to understand the dependence structure in a high-dimensional feature space has been well acknowledged in statistics literature since the last century ([16], [28]) due to its scalability and in some contexts brings more insight compared to the analysis of simple covariance matrix. For example, in human brain, two separate regions can be highly correlated with no direct relation and only due to their strong interaction with a common third region. So, understanding the conditional dependence structure and using it in clustering the brain regions is more informative in the context of understanding the functional connectivity in human brain [8]. Otherwise simple correlation based clustering will result in huge cluster sizes with less interpretable group of brain regions.

To this end, in order to estimate the precision matrix we implement nodewise Lasso algorithm [32] on the transformed variables $(\tilde{T}_y(Y), \tilde{T}_k(X_k))$, $k \in \hat{S}_n$. Nodewise Lasso regression is generally entertained to estimate a sparse precision matrix in the context of Gaussian graphical model by performing simultaneous Lasso regression on each predictor. The tuning parameters in each nodewise Lasso are typically selected using cross-validation. More details on this algorithm and their theoretical guarantees can be found in [23]. Let $\hat{\Sigma}^{-1}$ be the estimated precision matrix by the nodewise Lasso algorithm and $\rho(Z, Z')$ denotes any correlation metric for two random variables Z and Z' . Following Algorithm 1 summarizes the clustering step.

Here not only we are clustering the active predictors, but also select an appropriate representative from each cluster. First, for each active predictor $X_i \in \hat{S}_n$, we collect all the other active predictors conditionally dependent on X_i , and make cluster C_i . Although clustering using the conditional dependence produces smaller clusters, there might be some overlapping owing to the complex association in the original predictor space. Hence, to reduce the excessive intercluster correlation, we merge all those clusters having maximum correlation greater than some pre-specified threshold r (we typically set $r=0.9$). Next, each cluster is updated by adding all the other features conditionally dependent with the existing cluster members. Finally to find the appropriate cluster representatives, we focus on the HZ-test statistic \tilde{w}_k^* in 1 which measures the extend of resemblance between the distribution of each nonparametrically transformed variable in a cluster and the null distribution $N(0, I_2)$. So, for cluster C_i , we select the variable $R_i = \arg\max_{j \in C_i} \{\tilde{w}_j^*\}$ indicating its strongest association with the response variable compared to the other predictors in the cluster.

Algorithm 1: Finding clusters and the representatives

Input : $(X \in \mathcal{R}^{n \times p}, Y \in \mathcal{R}^n)$, The Active set \hat{S}_n , $|\hat{S}_n| = p_1 < p$

```

1 Estimate the precision matrix:  $\hat{\Sigma}^{-1} = (\hat{\sigma}^{ij})_{i,j \in \{1,2,\dots,p\}}$  using Nodewise Lasso
2 Define the clusters  $C_i = \{1 \leq j \leq p : \hat{\sigma}^{ij} \neq 0\}, i \in \hat{S}_n$ 
3 for  $1 \leq i \leq p_1$  do
4   for  $1 \leq j \leq p_1, j \neq i$  do
5     Define  $\Omega^{ij} = \{corr(X_{C_i}, X_{C_j})\} = \{\rho(X_l, X_{l'}) | l \in C_i, l' \in C_j\} \in \mathcal{R}^{|C_i||C_j|}$ 
6     if  $\max\{\Omega^{ij}\} \geq r$  then
7        $C_i = C_i \cup C_j$ 
8        $C_j = \phi$ 
9     end if
10   end for
11 end for
12 Retain only the non-null clusters:  $C = \{C_i : C_i \neq \phi, i \in \hat{S}_n\}$ 
13 Find the cluster representatives  $\tilde{S}_n = \{R_j, 1 \leq j \leq |C| : R_j = \arg\max_{l \in C_j} \{\tilde{w}_l^*\}\}$ 

```

Output : Clusters $C_1, C_2, \dots, C_{|C|}$ and corresponding cluster representatives $\tilde{S}_n = \{R_j, 1 \leq j \leq |C|\}$

2.2 Cleaning with DNN

We start this section with modeling the response Y and the cluster representatives $X_{\tilde{S}_n}$ obtained through 2.1.2. In order to perform the error controlled variable selection, each representative will be assigned an importance score followed by a resampling algorithm to finally control the FDR.

While it is possible to adopt any other generic sparsity inducing DNN procedure, here we focus on the LassoNet algorithm recently proposed by [18] for its elegant mathematical frameworks which naturally sets the stage for nonlinear feature selection. To approximate the unknown functional connection, it considers the class of all fully connected feed-forward residual neural networks; namely,

$$\mathcal{F} = \{f \equiv f_{\theta, W} : x \mapsto \theta^T x + h_W(x)\} \quad (3)$$

Here, W denotes the network parameters, K denotes the size of the first hidden layer, $W^{(0)} \in \mathcal{R}^{p \times K}$ denotes the first hidden layer parameters, $\theta \in \mathcal{R}^p$ denotes the residual layer's weights. In order to minimize the reconstruction error: the LassoNet objective function can be formulated as:

$$\min_{\theta, W} L(\theta, W) + \lambda \|\theta\|_1 \text{subject to } \|W_j^{(0)}\|_\infty \leq M|\theta_j|, j = 1, 2, \dots, p \quad (4)$$

With $L(\theta, W) = \frac{1}{n} \sum_{i=1}^n l(f_{\theta, W}(x_i), y_i)$ as the empirical loss on the training data and x_i as the vector of cluster representatives observed for the i^{th} individual. While the main feature sparsity is induced by the L_1 norm on residual layer parameter θ , the second constraint controls the total amount of nonlinearity of the predictors. As mentioned in [18], LassoNet can be argued as an extension of the celebrated Lasso algorithm to nonlinear variable selection.

In L_1 penalization framework, importance of a specific feature is naturally embedded into the highest penalization level upto which it can survive into the model. So, to measure the importance of each representative, the LassoNet algorithm is executed over a long range of tuning parameter $\lambda_1 \leq \lambda_2 \leq \dots \leq \lambda_r$ on $(Y, X_{\tilde{S}_n})$. In practice, a small value is fixed for λ_1 where all the variables are present in the model. Then we gradually increase the value of the tuning parameter and stop at λ_r , where there are no variables present in the model. Next the importance score for the j -th cluster is defined as $\hat{\lambda}_j = \max \lambda$ up to which the j -th representative exists in the model, and then the following rank statistic is computed: $\mathcal{I}_j = \sum_{j' \neq j} \mathbb{1}(\hat{\lambda}_j \leq \hat{\lambda}_{j'})$ for $j = 1, 2, \dots, |C|$. A lower \mathcal{I}_j means that the j -th cluster representative stays in the model upto a higher value λ implying its high potential as a significant cluster; whereas a higher \mathcal{I}_j indicates the corresponding cluster leaves the model even for a smaller value of λ as a consequence of being simply a collection of null features. Hence, we should only focus on the clusters with lower ranks. Additionally, in order to control the FDR, understanding the behaviour of the predictors under the null distribution is important. In traditional FDR controlling algorithms, this is typically done by generating the p-values. Here, as a p-value free algorithm, we propose the following resampling based approach:

1. Generate B bootstrap versions of the data $\left\{Y^b, X_{S_n}^b\right\}_{b=1}^B$ considering only the cluster representatives \tilde{S}_n . For each bootstrap version, run the LassoNet algorithm parallelly; and calculate the importance of each representative by measuring $\hat{\lambda}_j^b$ = maximum value of λ up to which the j -th predictor exists in the model for b -th bootstrap version, and then the ranks $\mathcal{I}_j^b = \sum_{j' \neq j} \mathbb{1}(\hat{\lambda}_j^b \leq \hat{\lambda}_{j'}^b)$. Therefore, the averaged rank is: $\bar{\mathcal{I}}_j = \frac{1}{B} \sum_{b=1}^B \mathcal{I}_j^b$
2. For an arbitrary threshold δ , we would select the cluster representatives with averaged rank $\bar{\mathcal{I}}_j$ lower than δ ; so we define, $N_+(\delta) = \sum_{j \in \tilde{S}_n} \mathbb{1}(\bar{\mathcal{I}}_j \leq \delta)$ representing the number of selected clusters with respect to the cutoff δ .
3. Next, to estimate the expected number of falsely discovered clusters, define $\mathcal{R}^b = \{j : \mathcal{I}_j^b \leq \delta\}$, the number of cluster representatives with higher importance score so that the corresponding rank is lower than the cutoff δ in the b -th bootstrap version. Additionally, define a neighbourhood $\mathcal{N}(\bar{\mathcal{I}}_j, \kappa) = \{l \in \{1, 2, \dots, |C|\} : |\bar{\mathcal{I}}_j - l| \leq \kappa\}$, for some specific small number κ .
4. Further, we estimate the number of falsely discovered clusters and hence an estimator of the FDR can be constructed as

$$\hat{e}_0(\delta) = \frac{1}{B} \sum_{b=1}^B \left\{ \sum_{j \in \mathcal{R}^b} \mathbb{1}(\mathcal{I}_j^b \notin \mathcal{N}(\bar{\mathcal{I}}_j, \kappa)) \right\} \text{ and } F\hat{D}R(\delta) = \frac{\hat{e}_0(\delta)}{N_+(\delta)} \quad (5)$$

5. The $F\hat{D}R$ is sequentially estimated with $\delta = \bar{\mathcal{I}}_{(1)}, \bar{\mathcal{I}}_{(2)}, \dots, \bar{\mathcal{I}}_{(|C|)}$ and the optimum threshold is $\Delta^* = \max\{\delta > 0 : F\hat{D}R(\delta) < q\}$ for some pre-specific FDR control level q . The final selected set of clusters with controlled FDR is given by $\hat{D}_n = \{C_j, j = 1, 2, \dots, |C| : \bar{\mathcal{I}}_j \leq \Delta^*\}$

The proposed method closely maintains all the flavours of an FDR-controlling approach. The notion of a false discovery is incorporated into the algorithm via the resampling: if a null predictor gets relatively higher importance score, that is most possibly due to that specific bootstrap version which creates the spurious relation, however, that would not be consistent for all the other bootstraps in general. On the other hand, all the bootstrap versions should consistently produce higher importance scores for the significant predictors. As a consequence, the variability in the ranks of the importance scores will be much higher for the null predictors compared to their nonnull counterpart. This notion has been introduced in the statistics literature few decades ago as bagging methods [4, 5] for reducing variance of a black-box prediction. The proposed method utilizes this phase transition in the feature selection framework to effectively identify the false discoveries; an empirical illustration of which is further provided in the section 2 of the SM.

3 Numerical Illustrations

3.1 Performance of existing feature selection methods in the presence of high multicollinearity

We first present a numerical illustration of performance of several recently proposed nonlinear FDR-controlled feature selection algorithms. The predictors are first generated from $X_i \sim N_p(0, \Sigma)$, $i = 1, 2, \dots, n$, for multiple combination of (n, p) and the covariance matrix Σ is chosen as a toeplitz matrix with $\Sigma_{ij} = \rho^{|i-j|}$, $\rho = 0.1, 0.5$, and 0.9 . Under simplistic setting, the response y is generated from $y = x_S \beta_S + \epsilon$, $S = \{5, 10, \dots, 50\}$, $|S| = 10$, with β_S generated from $N(\beta_0, 0.1)$ independently and $\beta_{S^c} = 0$. The random noise $\epsilon \sim N(0, 1)$. We focus on the Model-X knockoff [7], SurvNet [30], DeepPINK [22]. For a more rigorous analysis, we consider two different versions of Model-X knockoff - (1) Model-X-Estimated, where the knockoffs are generated using an estimated multivariate gaussian distribution and (2) Model-X-True, where the knockoffs are generated using the true data generating multivariate gaussian distribution mentioned above. For the knockoff generation, we consider the equicorrelated construction using the R package knockoff: The Knockoff Filter for Controlled Variable Selection. To implement the SurvNet and DeepPINK, we use the codes mentioned in the respective papers [30, 22]. We set $q = 0.15$ as the FDR control threshold.

Table 1 demonstrates that these algorithms are efficient and competitive given the availability of huge training data and moderate correlation among the features. However, under the current setting of low sample size with correlated features, they typically fail with lower power and excessive false discoveries. This is somehow expected, as these methods are not tailored for handing such huge multicollinearity. For example, both Model-X-Estimated and Model-X-True maintains the power-FDR balance under low correlation setup. However with higher multicollinearity, Model-X-Estimated

Table 1: Power and empirical FDR of various feature selection algorithms with standard error in parentheses

	(n, p)		$\beta = 2$			$\beta = 4$		
			$\rho = 0.1$	$\rho = 0.5$	$\rho = 0.9$	$\rho = 0.1$	$\rho = 0.5$	$\rho = 0.9$
Model-X-Estimated	(400, 1000)	Power	1.00 (0.00)	1.00 (0.00)	1.00 (0.00)	1.00 (0.00)	1.00 (0.00)	1.00 (0.00)
		FDR	0.13 (0.17)	0.12 (0.12)	0.27 (0.18)	0.11 (0.19)	0.20 (0.18)	0.27 (0.20)
Model-X-True	(400, 1000)	Power	1.00 (0.00)	1.00 (0.00)	1.00 (0.00)	1.00 (0.00)	1.00 (0.00)	1.00 (0.00)
		FDR	0.08 (0.13)	0.09 (0.12)	0.14 (0.17)	0.12 (0.14)	0.11 (0.13)	0.08 (0.12)
SurvNet	(400, 1000)	Power	0.27 (0.20)	0.32 (0.22)	0.35 (0.24)	0.49 (0.24)	0.52 (0.28)	0.58 (0.29)
		FDR	0.31 (0.36)	0.53 (0.30)	0.59 (0.23)	0.21 (0.21)	0.53 (0.18)	0.60 (0.17)
	(10000, 60)	Power	0.99 (0.05)	1.00 (0.00)	1.00 (0.00)	1.00 (0.00)	1.00 (0.00)	1.00 (0.00)
		FDR	0.20 (0.15)	0.80 (0.02)	0.78 (0.07)	0.14 (0.11)	0.80 (0.02)	0.56 (0.32)
DeepPINK	(400, 1000)	Power	0.01 (0.02)	0.03 (0.04)	0.00 (0.00)	0.03 (0.04)	0.01 (0.03)	0.02 (0.05)
		FDR	0.23 (0.40)	0.35 (0.42)	0.33 (0.47)	0.45 (0.44)	0.24 (0.41)	0.24 (0.40)
	(10000, 60)	Power	1.00 (0.00)	1.00 (0.00)	1.00 (0.00)	1.00 (0.00)	1.00 (0.00)	1.00 (0.00)
		FDR	0.18 (0.04)	0.29 (0.13)	0.25 (0.11)	0.17 (0.01)	0.24 (0.12)	0.24 (0.12)

fails to control the FDR below the specified threshold while the Model-X-True controls the FDR efficiently. This disparity indicates Model-X procedure induces inflation in false discoveries if the knockoffs are not generated properly under 'difficult' situation, as discussed in [1]. As expected, the DL-based algorithms, such as SurvNet and DeepPINK work much better in big-n-small-p and low correlation setup but typically fail in other cases, indicating their reduced effectiveness in ultrahigh dimensional data with small sample size. This pivot analysis further motivates the need for the cluster-level feature discovery following a screening step and set the stage for the proposed method SciDNet.

3.2 Empirical performance of SciDNet

In this section, to demonstrate the finite-sample performance of SciDNet, we consider a wide spectrum of simulation scenarios. The performance is analyzed from two perspectives: feature selection performance (in table 2) as well as prediction accuracy (in table 3).

Single Index models are straightforward yet flexible example of nonlinear models where the response is related to a linear combination of the features through an unknown nonlinear, monotonic link function, i.e. $y = g(x'\beta) + \epsilon$. Here we choose the following two link functions as our data generating process: (1) **Polynomial**: $g(x) = \frac{x^3}{10} + 3\frac{x}{10}$ and (2) **ReLU**: $g(x) = \max(0, x)$.

We set $n = 400$ and $p = 1000$. The coefficients $\beta \in \mathcal{R}^p$ is sparse with the true nonzero locations $S = \{50, 100, 150, 200, 250\}$, where $\beta_{S^c} = 0, \beta_S \sim N_S(u\beta_0, 0.1)$ with $u = \{\pm 1\}^S$. The value of β_0 is set as $\beta_0 = 2, 4$ to incorporate varying signal strength. The random error $\epsilon \sim N(0, \sigma^2)$, with three increasing noise level as $\sigma^2 = 1, 5, 10$. The high dimensional predictors are generated from $X \sim N_p(0, \Sigma)$ where the covariance matrix Σ is chosen as a toeplitz matrix with $\Sigma_{ij} = \rho^{|i-j|}$. We set $\rho = 0.95$.

We consider the performance of SciDNet with the basic LassoNet algorithm. The results clearly indicate the need for a 'cleaning' while using a DL model for feature selection. Table 2 illustrates that the proposed method SciDNet enjoys quick recovery in power while we gradually increase the error-controlling threshold q from 0.01 to 0.15 while maintaining the number of false discoveries below the required level. We further implemented two DL-based predictive model on the features selected by SciDNet - (1) an MLP - a feed forward neural network with 2 hidden layers and (2) LassoNet. The reward for the successful feature selection by SciDNet is further indicated in table 3 by the huge gain in test accuracy observed with a lower Mean Square Error (MSE) on the test data.

Further simulation study is conducted considering various nonlinear models as data generating process and the results are presented in the section 2 of the supplementary material. SciDNet continues to maintain the satisfactory power-FDR balance for various models with and without interaction terms.

4 Real Data Analysis

In addition to the simulation studies, we implemented the proposed algorithm in the context of riboflavin (vitamin B2) production with *bacillus subtilis* data, a publicly accessible dataset available in the 'hdi' package in R. Here the continuous response is the logarithm of the riboflavin production rate, observed for $n = 71$ samples along with

Table 2: Power and empirical FDR with standard error in parentheses showing the feature selection performance

FDR control Level q		$\beta = 2$				LassoNet	$\beta = 4$				LassoNet		
		SciDNet					SciDNet						
		0.01	0.05	0.1	0.15		0.01	0.05	0.1	0.15			
Polynomial	$\sigma^2 = 1$	Power	0.59 (0.17)	0.97 (0.06)	0.98 (0.05)	0.98 (0.05)	0.33 (0.14)	0.72 (0.32)	0.91 (0.12)	0.97 (0.07)	0.98 (0.05)	0.27 (0.17)	
		FDR	0.01 (0.02)	0.02 (0.04)	0.04 (0.06)	0.10 (0.05)	0.94 (0.02)	0.01 (0.02)	0.01 (0.03)	0.02 (0.04)	0.05 (0.06)	0.95 (0.03)	
	$\sigma^2 = 5$	Power	0.47 (0.27)	0.80 (0.20)	0.86 (0.13)	0.88 (0.12)	0.33 (0.10)	0.56 (0.27)	0.82 (0.19)	0.93 (0.09)	0.95 (0.08)	0.36 (0.17)	
		FDR	0.00 (0.00)	0.04 (0.06)	0.09 (0.07)	0.12 (0.08)	0.95 (0.02)	0.00 (0.00)	0.01 (0.04)	0.04 (0.06)	0.06 (0.07)	0.92 (0.04)	
	$\sigma^2 = 10$	Power	0.28 (0.21)	0.55 (0.25)	0.65 (0.20)	0.71 (0.18)	0.27 (0.22)	0.40 (0.35)	0.86 (0.14)	0.92 (0.10)	0.93 (0.08)	0.29 (0.15)	
		FDR	0.00 (0.00)	0.03 (0.05)	0.11 (0.09)	0.15 (0.11)	0.96 (0.03)	0.00 (0.00)	0.02 (0.04)	0.04 (0.05)	0.07 (0.06)	0.94 (0.03)	
ReLU	$\sigma^2 = 1$	Power	0.63 (0.36)	0.90 (0.16)	0.97 (0.06)	0.98 (0.05)	0.75 (0.19)	0.65 (0.38)	0.96 (0.07)	0.97 (0.07)	0.98 (0.05)	0.81 (0.16)	
		FDR	0.00 (0.00)	0.02 (0.05)	0.05 (0.06)	0.09 (0.07)	0.92 (0.02)	0.01 (0.03)	0.05 (0.05)	0.08 (0.06)	0.12 (0.06)	0.90 (0.02)	
	$\sigma^2 = 5$	Power	0.55 (0.22)	0.82 (0.14)	0.89 (0.10)	0.90 (0.10)	0.48 (0.26)	0.61 (0.32)	0.91 (0.14)	0.95 (0.10)	0.96 (0.09)	0.73 (0.17)	
		FDR	0.00 (0.02)	0.04 (0.06)	0.10 (0.09)	0.14 (0.09)	0.95 (0.02)	0.00 (0.02)	0.02 (0.04)	0.06 (0.06)	0.10 (0.08)	0.93 (0.01)	
	$\sigma^2 = 10$	Power	0.37 (0.23)	0.62 (0.22)	0.74 (0.15)	0.79 (0.13)	0.45 (0.28)	0.65 (0.32)	0.90 (0.11)	0.94 (0.08)	0.95 (0.08)	0.68 (0.23)	
		FDR	0.01 (0.04)	0.06 (0.08)	0.08 (0.11)	0.14 (0.13)	0.96 (0.02)	0.01 (0.03)	0.05 (0.06)	0.11 (0.06)	0.14 (0.08)	0.95 (0.02)	

Table 3: Test MSE with standard error in parentheses showing the prediction performance before and after the feature selection

		$\beta = 2$					$\beta = 4$				
		MLP	SciDNet+MLP	LassoNet	SciDNet+LassoNet		MLP	SciDNet+MLP	LassoNet	SciDNet+FS	
Polynomial	$\sigma^2 = 1$	3.587 (2.265)	0.033 (0.018)	0.340 (0.186)	0.335 (0.194)		4.244 (2.509)	0.058 (0.060)	0.367 (0.192)	0.367 (0.194)	
	$\sigma^2 = 5$	4.283 (3.101)	0.044 (0.021)	0.524 (0.011)	0.505 (0.109)		4.569 (2.627)	0.049 (0.044)	0.295 (0.187)	0.292 (0.183)	
	$\sigma^2 = 10$	4.213 (2.980)	0.044 (0.012)	0.723 (0.113)	0.712 (0.125)		5.192 (2.618)	0.050 (0.039)	0.320 (0.163)	0.320 (0.157)	
ReLU	$\sigma^2 = 1$	4.507 (2.879)	0.051 (0.017)	0.209 (0.048)	0.204 (0.098)		4.271 (2.261)	0.048 (0.019)	0.120 (0.027)	0.109 (0.031)	
	$\sigma^2 = 5$	3.532 (1.929)	0.045 (0.020)	0.518 (0.082)	0.512 (0.155)		4.488 (2.044)	0.047 (0.014)	0.273 (0.085)	0.226 (0.087)	
	$\sigma^2 = 10$	4.557 (3.357)	0.046 (0.011)	0.689 (0.148)	0.631 (0.132)		3.926 (3.062)	0.047 (0.016)	0.347 (0.064)	0.312 (0.118)	

$p = 4088$ predictors which are the logarithm of the expression level of 4088 genes. In order to understand which genes are important for the riboflavin production, SciDNet resulted in finding 9 clusters of correlated genes at the 15% FDR control level. Similar to the simulation studies in 3, as a validation of discovering the meaningful clusters, we compute the test MSE by fitting two predictive DL models (the MLP and the LassoNet) on the cluster of genes discovered by SciDNet. To overcome the extra burden of the low sample size and ultrahigh dimensionality in this data, we consider 50 independent replications in the test MSE calculation step. In each replication, the data is divided into training and testing maintaining 8 : 2 ratio to get the test MSE and the final estimate is obtained by averaging all the test MSE's calculated on each these replications.

Additionally, for comparing the performance of SciDNet, we mention test MSE obtained by applying other ML algorithms originally proposed for simultaneous feature selection and prediction such as (1) cross-validated LassoNet, (2) ENNS algorithm coupled with a l_1 regularized neural network [36], (3) the sparse group lasso penalized neural network [11], (3) lasso penalized linear regression, and (4) the group lasso penalized generalized additive model [37]. More elaborate implementation details of these additional algorithms can be obtained at [36]. Table 4 demonstrates the gain of SciDNet by achieving the lowest prediction error. This behaviour is consistent with the simulation study and consolidates the need for applying an apt feature selection method prior to fit a predictive model for an explainable research outcome. The list of selected cluster of genes by SciDNet are relegated to the section 5 of the supplementary material.

Table 4: Test MSE with standard error in parentheses for different DL-based models applied in the riboflavin gene data example

Algorithm	Test MSE
SciDNet + LassoNet	0.124 (0.118)
SciDNet + MLP	0.219 (0.123)
LassoNet	0.176 (0.148)
ENNS+ l_1 neural network	0.268 (0.115)
Regularized neural network	0.273 (0.135)
Linear model with LASSO	0.286 (0.124)
Generalized additive model with group lasso	0.282 (0.136)

5 Discussion

While the explainable AI is the need of the hour, statistical models coupled with cutting-edge ML techniques have to push forward because of their solid theoretical foundation clipped with principled algorithmic advancement. The proposed method SciDNet efficiently exploits several existing tools in statistics and ML literature to circumvent some of the complexities that current DL-based models fail to address properly. It provides an end-to-end framework for error-controlled feature selection in ultrahigh dimensional datasets with the presence of severe multicollinearity in the feature space. SciDNet effectively maintains its performance at the cost of multi-resolution discovery sets by properly utilizing the accumulated information generated from the resampling. Our empirical study demonstrates that a black-box predictive model produces more accurate results when applied to the features selected by SciDNet rather than its implementation on the whole feature space; indicating the proposed algorithm's potential use in both feature selection and prediction. Due to the screening step, SciDNet is scalable and the resampling part can be easily implemented as parallel chains for faster computation.

There is a large class of DNN available in the literature and widely applied to various applications. However, very few of them can be directly applicable to the setting we consider in this paper. The basic intuition and exciting empirical results of SciDNet on simulated and real datasets encourage further research in multiple directions. One would be interested in developing a theoretical foundation of this 'screening' and 'cleaning' strategy for provable FDR control. It would be worth mentioning that although we used the sure independence screening with HZ-test and LassoNet as the main tools, SciDNet puts forward a more generic framework and can be implemented with any other model-free feature screening method and sparsity-inducing DL algorithms like [11]. In the screening part, we consider the use of sparse precision matrix for clustering the features as it is easier to estimate when combined with the nonparanormal transformation and nodewise lasso algorithm. Although this is justified as the nonparanormal preserves the conditional dependency structure under mild assumptions [20], further methodological extension would focus on another approach for capturing the correlation directly in the active predictors. Additionally, after the screening step, the dimensionality is reduced, it would be interesting to implement a model-free knockoff generating algorithms like [24] in the cleaning step as further algorithmic development. One limitation is that we mainly focus on the regression setup with the continuous outcome because of the requirements of Henze–Zirkler sure Independence test used in the screening step. Further research should be conducted for extending SciDNet to classification problems as well.

References

- [1] Rina Foygel Barber, Emmanuel J Candès, and Richard J Samworth. Robust inference with knockoffs. *The Annals of Statistics*, 48(3):1409–1431, 2020.
- [2] Yoav Benjamini and Yosef Hochberg. Controlling the false discovery rate: a practical and powerful approach to multiple testing. *Journal of the Royal Statistical society: series B (Methodological)*, 57(1):289–300, 1995.
- [3] Peter Bickel, Peter Bühlmann, Qiwei Yao, Richard Samworth, Peter Hall, DM Titterington, Jing-Hao Xue, C Anagnostopoulos, DK Tasoulis, Wenyang Zhang, et al. Sure independence screening for ultrahigh dimensional feature space discussion. *Journal of the Royal Statistical Society. Series B, Statistical Methodology*, 70(5):883–911, 2008.
- [4] Leo Breiman. Bagging predictors. *Machine learning*, 24(2):123–140, 1996.
- [5] Peter Bühlmann and Bin Yu. Analyzing bagging. *The Annals of Statistics*, 30(4):927 – 961, 2002. doi: 10.1214/aoas/1031689014. URL <https://doi.org/10.1214/aoas/1031689014>.
- [6] Peter Bühlmann, Markus Kalisch, and Lukas Meier. High-dimensional statistics with a view toward applications in biology. *Annual Review of Statistics and Its Application*, 1(1):255–278, 2014. doi: 10.1146/annurev-statistics-022513-115545. URL <https://doi.org/10.1146/annurev-statistics-022513-115545>.
- [7] Emmanuel J. Candès, Yingying Fan, Lucas Janson, and Jinchi Lv. Panning for gold: Model-x knockoffs for high-dimensional controlled variable selection. *arXiv: Methodology*, 2016.
- [8] Anup Das, Aaron L. Sampson, Claudia Lainscsek, Lyle Muller, Wutu Lin, John C. Doyle, Sydney S. Cash, Eric Halgren, and Terrence J. Sejnowski. Interpretation of the Precision Matrix and Its Application in Estimating Sparse Brain Connectivity during Sleep Spindles from Human Electrocorticography Recordings. *Neural Computation*, 29(3):603–642, 03 2017. ISSN 0899-7667. doi: 10.1162/NECO_a_00936. URL https://doi.org/10.1162/NECO_a_00936.
- [9] Dennis Elbrächter, Dmytro Perekrestenko, Philipp Grohs, and Helmut Bölcskei. Deep neural network approximation theory. *IEEE Transactions on Information Theory*, 67(5):2581–2623, 2021.

- [10] Jianqing Fan and Jinchi Lv. A selective overview of variable selection in high dimensional feature space. *Statistica Sinica*, 20(1):101, 2010.
- [11] Jean Feng and Noah Simon. Sparse-input neural networks for high-dimensional nonparametric regression and classification. *arXiv preprint arXiv:1711.07592*, 2017.
- [12] Amirata Ghorbani, Abubakar Abid, and James Zou. Interpretation of neural networks is fragile. In *Proceedings of the AAAI conference on artificial intelligence*, volume 33, pages 3681–3688, 2019.
- [13] N. Henze and B. Zirkler. A class of invariant consistent tests for multivariate normality. *Communications in Statistics - Theory and Methods*, 19(10):3595–3617, 1990. doi: 10.1080/03610929008830400. URL <https://doi.org/10.1080/03610929008830400>.
- [14] Farhad Hormozdiari, Emrah Kostem, Eun Yong Kang, Bogdan Pasaniuc, and Eleazar Eskin. Identifying causal variants at loci with multiple signals of association. *Genetics*, 198(2):497–508, 2014.
- [15] James Jordon, Jinsung Yoon, and Mihaela van der Schaar. KnockoffGAN: Generating knockoffs for feature selection using generative adversarial networks. In *International Conference on Learning Representations*, 2019. URL <https://openreview.net/forum?id=ByeZ5jC5YQ>.
- [16] Steffen L Lauritzen. *Graphical models*, volume 17. Clarendon Press, 1996.
- [17] Lihua Lei and William Fithian. Adapt: an interactive procedure for multiple testing with side information. *Journal of the Royal Statistical Society: Series B (Statistical Methodology)*, 80(4):649–679, 2018. doi: <https://doi.org/10.1111/rssb.12274>. URL <https://rss.onlinelibrary.wiley.com/doi/abs/10.1111/rssb.12274>.
- [18] Ismael Lemhadri, Feng Ruan, Louis Abraham, and Robert Tibshirani. Lassonet: A neural network with feature sparsity. *Journal of Machine Learning Research*, 22(127):1–29, 2021. URL <http://jmlr.org/papers/v22/20-848.html>.
- [19] Ang Li and Rina Foygel Barber. Multiple testing with the structure-adaptive benjamini–hochberg algorithm. *Journal of the Royal Statistical Society: Series B (Statistical Methodology)*, 81(1):45–74, 2019.
- [20] Han Liu, John Lafferty, and Larry Wasserman. The nonparanormal: Semiparametric estimation of high dimensional undirected graphs. *Journal of Machine Learning Research*, 10(10), 2009.
- [21] Ying Liu and Cheng Zheng. Deep latent variable models for generating knockoffs. *Stat*, 8(1):e260, 2019.
- [22] Yang Lu, Yingying Fan, Jinchi Lv, and William Stafford Noble. Deeppink: reproducible feature selection in deep neural networks. In S. Bengio, H. Wallach, H. Larochelle, K. Grauman, N. Cesa-Bianchi, and R. Garnett, editors, *Advances in Neural Information Processing Systems*, volume 31. Curran Associates, Inc., 2018. URL <https://proceedings.neurips.cc/paper/2018/file/29daf9442f3c0b60642b14c081b4a556-Paper.pdf>.
- [23] Nicolai Meinshausen and Peter Bühlmann. High-dimensional graphs and variable selection with the Lasso. *The Annals of Statistics*, 34(3):1436 – 1462, 2006. doi: 10.1214/009053606000000281. URL <https://doi.org/10.1214/009053606000000281>.
- [24] Yaniv Romano, Matteo Sesia, and Emmanuel Candès. Deep knockoffs. *Journal of the American Statistical Association*, 115(532):1861–1872, 2020. doi: 10.1080/01621459.2019.1660174. URL <https://doi.org/10.1080/01621459.2019.1660174>.
- [25] Cynthia Rudin. Stop explaining black box machine learning models for high stakes decisions and use interpretable models instead. *Nature Machine Intelligence*, 1(5):206–215, 2019.
- [26] M Sesia, C Sabatti, and E J Candès. Gene hunting with hidden Markov model knockoffs. *Biometrika*, 106(1):1–18, 08 2018. ISSN 0006-3444. doi: 10.1093/biomet/asy033. URL <https://doi.org/10.1093/biomet/asy033>.
- [27] Matteo Sesia, Eugene Katsevich, Stephen Bates, Emmanuel Candès, and Chiara Sabatti. Multi-resolution localization of causal variants across the genome. *bioRxiv*, 2019. doi: 10.1101/631390. URL <https://www.biorxiv.org/content/early/2019/05/24/631390>.
- [28] Ali Shojaie and George Michailidis. Penalized likelihood methods for estimation of sparse high-dimensional directed acyclic graphs. *Biometrika*, 97(3):519–538, 2010.
- [29] David O Siegmund, Nancy R Zhang, and Benjamin Yakir. False discovery rate for scanning statistics. *Biometrika*, 98(4):979–985, 2011.
- [30] Zixuan Song and Jun Li. Variable selection with false discovery rate control in deep neural networks. *Nature Machine Intelligence*, 3(5):426–433, 2021.
- [31] Wesley Tansey, Yixin Wang, David Blei, and Raul Rabadian. Black box FDR. In Jennifer Dy and Andreas Krause, editors, *Proceedings of the 35th International Conference on Machine Learning*, volume 80 of *Proceedings of Machine Learning Research*, pages 4867–4876. PMLR, 10–15 Jul 2018. URL <https://proceedings.mlr.press/v80/tansey18a.html>.

- [32] Sara Van de Geer, Peter Bühlmann, Ya'acov Ritov, and Ruben Dezeure. On asymptotically optimal confidence regions and tests for high-dimensional models. *The Annals of Statistics*, 42(3):1166–1202, 2014.
- [33] Gao Wang, Abhishek Sarkar, Peter Carbonetto, and Matthew Stephens. A simple new approach to variable selection in regression, with application to genetic fine-mapping. *bioRxiv*, 2020. doi: 10.1101/501114. URL <https://www.biorxiv.org/content/early/2020/06/27/501114>.
- [34] F. Xia, Martin Jinye Zhang, James Y. Zou, and David Tse. Neuralfdr: Learning discovery thresholds from hypothesis features. In *NIPS*, 2017.
- [35] Jingnan Xue and Faming Liang. A robust model-free feature screening method for ultrahigh-dimensional data. *Journal of Computational and Graphical Statistics*, 26(4):803–813, 2017.
- [36] Kaixu Yang and Tapabrata Maiti. Enns: Variable selection, regression, classification and deep neural network for high-dimensional data. *arXiv preprint arXiv:2107.03430*, 2021.
- [37] Kaixu Yang and Tapabrata Maiti. Ultrahigh-dimensional generalized additive model: Unified theory and methods. *Scandinavian Journal of Statistics*, 2021.

Appendix

A Some Technical Details

In this section, elaborate comment on some technical and implementation details on the proposed algorithm SciDNet is discussed.

A.0.1 Controlling an upper bound of the FDR

Now we will provide the reason for controlling $\frac{E(e_0)}{N_+}$, by showing this random quantity can be treated as an upper bound of $\text{FDP} = \frac{e_0}{N_+}$, where for cutoff δ , $e_0 = \#\{j \notin S : \bar{I}_j \geq \delta\}$ and $N_+ = \#\{j \ni S : \bar{I}_j \geq \delta\}$.

We first start with defining T as the number of true discoveries, i.e., $T = \#\{j \in S : \bar{I}_j \geq \delta\}$ and

$$FDR = E\left(\frac{e_0}{N_+}\right) = E\left(\frac{e_0}{e_0 + T}\right) = E\left[E\left(\frac{e_0}{e_0 + T} \mid T\right)\right] \leq E\left[\frac{E(e_0 \mid T)}{E(e_0 \mid T) + T}\right] \quad (6)$$

The last inequality can be obtained by applying conditional Jensen's inequality to the concave function $f(x) = \frac{x}{x+t}$, for $t > 0$. Now, to show $\frac{E(e_0)}{N_+}$ as an upper bound of the FDP, we proceed as follows:

$$\begin{aligned} E\left[\frac{E(e_0)}{N_+}\right] &= E(e_0)E\left(\frac{1}{e_0 + T}\right) = E(e_0)E\left[E\left(\frac{1}{e_0 + T} \mid T\right)\right] \geq E(e_0)E\left(\frac{1}{E(e_0 \mid T) + T}\right) \\ &= E(E(e_0 \mid T))E\left(\frac{1}{E(e_0 \mid T) + T}\right) \\ &\geq E\left(\frac{E(e_0 \mid T)}{E(e_0 \mid T) + T}\right) \geq FDR \end{aligned} \quad (7)$$

While the first inequality in (7) can be obtained by applying conditional Jensen's inequality again to the convex function $f(x) = \frac{1}{x}$ and the third inequality is from (6); the second inequality can be justified under the assumption $\text{cov}(E(e_0 \mid T), \frac{1}{E(e_0 \mid T) + T}) \leq 0 \Rightarrow \text{cov}(E(e_0 \mid T), \frac{1}{E(N_+ \mid T)}) \leq 0$. This assumption is fairly intuitive too, stating that conditional on the number of true discoveries, the number of false discoveries and inverse of the number of total discoveries should be negatively correlated.

A.0.2 The estimate of the expected number of false discoveries $E(e_0)$

At the screening step, the clusters $C_1, C_2, \dots, C_{|C|}$ are formed in such a way that the intra-cluster correlations are not high and thus the cluster representatives are weakly correlated among themselves. So, analogous to p-value, for

unimportant clusters, the important scores will closely follow an uniform distribution. Assuming that $|S_0| = s$,

$$\begin{aligned}
e_0(\delta) &= \text{Expected number of false discoveries wrt cutoff } \delta \\
&= E \left(\sum_{j=1}^{|C|} \mathbb{1} (\bar{\mathcal{I}}_j \leq \delta, j \in S_0^c \cap \tilde{S}_n) \right) \\
&\leq E \left(\sum_{j=1}^{|C|} \mathbb{1} (\bar{\mathcal{I}}_j \leq \delta, \mathcal{I}_j^b \sim U(s+1, |C|)) \right) \text{ for any } b = 1, 2, \dots, B \\
&= E \left(\sum_{j=1}^{|C|} \mathbb{1} (\bar{\mathcal{I}}_j \leq \delta, \mathcal{I}_j^b \sim U(s+1, |C|), \mathcal{I}_j^b \in \mathcal{N}(\bar{\mathcal{I}}_j, \kappa)) \right) + \\
&\quad E \left(\sum_{j=1}^{|C|} \mathbb{1} (\bar{\mathcal{I}}_j \leq \delta, \mathcal{I}_j^b \sim U(s+1, |C|), \mathcal{I}_j^b \notin \mathcal{N}(\bar{\mathcal{I}}_j, \kappa)) \right) \\
&\leq 2 * E \left(\sum_{j=1}^{|C|} \mathbb{1} (\bar{\mathcal{I}}_j \leq \delta, \mathcal{I}_j^b \sim U(s+1, |C|), \mathcal{I}_j^b \notin \mathcal{N}(\bar{\mathcal{I}}_j, \kappa)) \right) \\
&\triangleq \frac{2}{B} \sum_{b=1}^B \left\{ \sum_{j \in \mathcal{R}^b} \mathbb{1} (\mathcal{I}_j^b \notin \mathcal{N}(\bar{\mathcal{I}}_j, \kappa)) \right\}
\end{aligned} \tag{8}$$

Explanation of these notations can be found at section 2 of the main manuscript.

A.0.3 Hyperparameter Selection

Recently developed Deep Learning (DL) models are generally governed by several hyperparameters and properly tuning them is necessary to get effective results. The proposed SciDNet relies on the following hyperparameters: (1) size of the active set \hat{S}_n , (2) the intracluster correlation bound r , (3) LassoNet tuning parameters λ and M and (4) κ used in neighbourhood selection in cleaning step. SciDNet is fairly robust to most of the associated hyperparameters. We discuss a practical way to tune all these hyperparameters here:

1. To choose the size of the active set, we propose to select a bigger active set with size proportional to $\nu_n = [n/\log(n)]$. As we further cluster the active variables in the clustering step, a slightly bigger active set with boost up the confidence of sure screening property, See the section C for an example.
2. After clustering, the intra-cluster correlation bound r should be fixed at some higher value (usually at 0.9 or 0.95) otherwise the cluster sizes will be inflated.
3. In cleaning step, a thorough grid search has been done over λ considering $\lambda_1 \leq \lambda_2 \leq \dots \leq \lambda_r$; in practice, a small value is fixed for λ_1 where all the variables are present in the model. Then the value of the tuning parameter gradually increased up to λ_r , where there are no variables present in the model. The other hyperparameter for LassoNet is the hierarchy coefficient M for which we follow the path considered in [18] and set $M = 10$. However, a more flexible approach would be a parallel grid search for M as well.
4. Finally, choosing an appropriate value of κ has a significant effect on the performance of SciDNet. The higher value of κ might lead to weaker control over the inclusion of false discoveries, whereas choosing a small κ will stricten the error control resulting in reduced power. However, we propose an effective way to tune the κ with the assist of phase transition in the ranks of the importance score \mathcal{I}_j of the cluster representatives. For an illustration, in Figure 1 a simple nonlinear additive model (see section B.1 for more details of the model) is considered with 122 active representatives obtained from the screening step. The first 5 representative features are significant (indicated by the dotted red line) and the ranks of their importance scores are presented along the y-axis. Here the dense lines are the bootstrap ranks \mathcal{I}_j^b , observed at 50 bootstrap replications and the solid blue line represents their averaged rank $\bar{\mathcal{I}}_j$ for all the 122 predictors. One would observe a clear phase transition in the bootstrap distribution of the ranks. For the significant features, the ranks are lower with extremely precise estimates whereas for the rest of the features, the averaged ranks posses much higher values coupled with huge variability. Hence, for a compact neighbourhood $\mathcal{N}(\bar{\mathcal{I}}_j, \kappa)$ to capture only the small variability in the bootstrap ranks of the significant features, we simply fix $\kappa = \mathbf{K}^*$ (in figure 1), the phase transition point for the averaged rank.

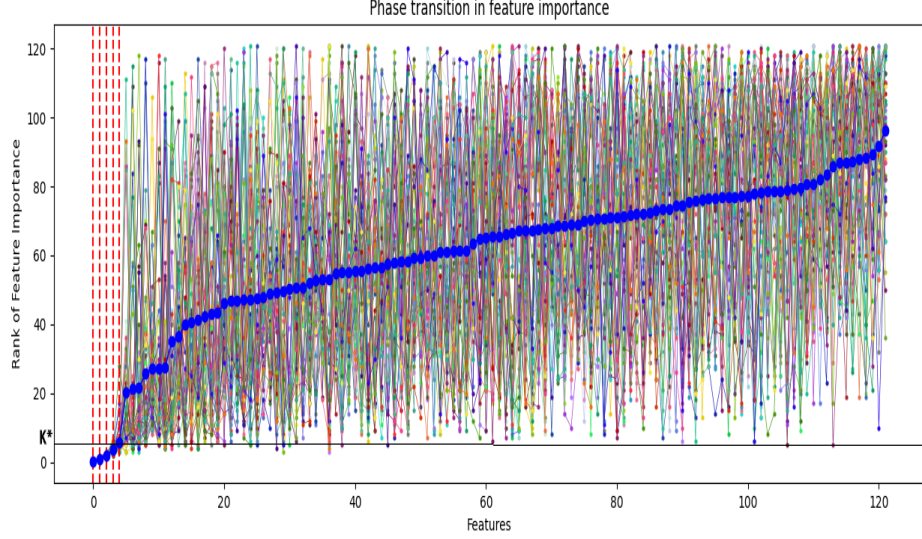


Figure 1: Illustration of phase transition in ranks of feature importance scores

Table A5: Power and empirical FDR of SciDNet with standard error in parentheses for gaussian features

ρ	snr	q	Nonlinear Additive				Nonlinear with interaction				Linear				
			0.01	0.05	0.1	0.15	0.01	0.05	0.1	0.15	0.01	0.05	0.1	0.15	
$\rho = 0.9$	$snr = 9 : 1$	Power	0.79 (0.19)	0.93 (0.11)	0.96 (0.09)	0.96 (0.09)	0.99 (0.06)	1.00 (0.00)	1.00 (0.00)	1.00 (0.00)	1.00 (0.00)	1.00 (0.00)	1.00 (0.00)	1.00 (0.00)	
		FDR	0.00 (0.00)	0.00 (0.02)	0.01 (0.03)	0.02 (0.05)	0.00 (0.00)	0.02 (0.05)	0.03 (0.06)	0.04 (0.08)	0.00 (0.00)	0.01 (0.04)	0.01 (0.05)	0.01 (0.05)	
	$snr = 8 : 2$	Power	0.59 (0.20)	0.82 (0.15)	0.86 (0.14)	0.87 (0.13)	0.84 (0.24)	1.00 (0.03)	1.00 (0.03)	1.00 (0.03)	1.00 (0.00)	1.00 (0.00)	1.00 (0.00)	1.00 (0.00)	
		FDR	0.00 (0.03)	0.00 (0.03)	0.03 (0.07)	0.04 (0.08)	0.00 (0.00)	0.01 (0.03)	0.02 (0.06)	0.04 (0.07)	0.01 (0.05)	0.02 (0.06)	0.02 (0.06)	0.02 (0.06)	
	$snr = 7 : 3$	Power	0.42 (0.20)	0.65 (0.12)	0.77 (0.14)	0.81 (0.14)	0.72 (0.26)	0.94 (0.12)	0.95 (0.12)	0.96 (0.11)	1.00 (0.00)	1.00 (0.00)	1.00 (0.00)	1.00 (0.00)	
		FDR	0.00 (0.00)	0.00 (0.00)	0.00 (0.03)	0.01 (0.05)	0.01 (0.04)	0.03 (0.06)	0.03 (0.07)	0.05 (0.09)	0.00 (0.02)	0.02 (0.05)	0.02 (0.05)	0.02 (0.06)	
	$\rho = 0.95$	$snr = 9 : 1$	Power	0.83 (0.18)	0.96 (0.08)	0.98 (0.06)	0.98 (0.06)	0.99 (0.04)	1.00 (0.00)	1.00 (0.00)	1.00 (0.00)	1.00 (0.00)	1.00 (0.00)	1.00 (0.00)	1.00 (0.00)
		$snr = 8 : 2$	Power	0.60 (0.29)	0.82 (0.17)	0.87 (0.14)	0.89 (0.12)	0.98 (0.08)	0.99 (0.05)	0.99 (0.05)	0.99 (0.05)	1.00 (0.00)	1.00 (0.00)	1.00 (0.00)	1.00 (0.00)
		$snr = 7 : 3$	Power	0.32 (0.22)	0.61 (0.19)	0.79 (0.15)	0.82 (0.15)	0.80 (0.27)	0.96 (0.11)	0.98 (0.05)	0.98 (0.05)	0.93 (0.19)	0.96 (0.11)	0.97 (0.09)	0.97 (0.09)
		FDR	0.00 (0.00)	0.01 (0.04)	0.01 (0.05)	0.03 (0.08)	0.00 (0.02)	0.04 (0.07)	0.07 (0.09)	0.12 (0.10)	0.00 (0.03)	0.04 (0.08)	0.06 (0.08)	0.07 (0.09)	

B More Simulation Results

Here we demonstrate finite sample performance of SciDNet under various linear and nonlinear models with varying multicollinearity level under different signal-to-noise-ratio.

B.1 Using Gaussian Features

For the high dimensional predictors, n i.i.d. copies are first generated from $X \sim N_p(0, \Sigma)$, where $n = 600$, $p = 5000$ and the covariance matrix Σ is chosen as a toeplitz matrix with $\Sigma_{ij} = \rho^{|i-j|}$. The value of ρ is varied to explore different correlation strength. We set the set of truly significant variables $S = \{100, 200, 300, 400, 500\}$ with $s = 5$. The response y is generated from $y = g(x) + \epsilon$. Here we entertain the following three models:

1. **Linear:** $g(x) = x_S \beta_S$ with β_S generated from $N(2, 0.1)$ independently and $\beta_{S^c} = 0$,
2. **Nonlinear additive:** $g(x) = 2x_{100} + 2x_{200}^3 + e^{x_{300}} + 6 \sin x_{400} + 2 \text{ReLU}(x_{500}^3)$, where $\text{ReLU}(x) = \max(x, 0)$
3. **Nonlinear with interaction:** $g(x) = 2x_{100} + 2x_{200}^3 + e^{x_{300}} + 6x_{400}x_{500}$

In each cases, the random noise ϵ is independently generated from $N(0, \sigma^2)$, where the value of σ^2 is chosen maintaining the signal-to-noise ratio at the desired level. To this end, we define the signal-to-noise ratio as $snr = \frac{\text{var}(g(x))}{\sigma^2}$. Here we consider three levels of $snr = 9 : 1, 8 : 2$ and $7 : 3$. Table A5 shows that SciDNet continues to maintain satisfactory power while successfully controlling the FDR below the threshold $q = 0.01, 0.05, 0.1, 0.15$. The average cluster size is observed at 8.3 for $\rho = 0.9$ and 13.4 for $\rho = 0.95$.

B.2 Using Non-gaussian Features

To check SciDNet's performance under non-gaussian setup, n iid copies of high-dimensional feature vector \mathbf{X} are generated from multivariate $t_p(5)$ distribution with $n=600$, $p=5000$. The remaining simulation setting is consistent with the previous section 2.1. The performance of SciDNet is presented at table A6 which is quite analogous to the results of gaussian features.

Table A6: Power and empirical FDR of SciDNet with standard error in parentheses for non-gaussian features

ρ	snr	q	Nonlinear Additive				Nonlinear with interaction				Linear			
			0.01	0.05	0.1	0.15	0.01	0.05	0.1	0.15	0.01	0.05	0.1	0.15
$\rho = 0.9$	$snr = 9 : 1$	Power	0.68 (0.12)	0.96 (0.15)	1.00 (0.09)	1.00 (0.07)	0.92 (0.05)	0.95 (0.02)	1.00 (0.00)	1.00 (0.00)	1.00 (0.00)	1.00 (0.00)	1.00 (0.00)	1.00 (0.00)
		FDR	0.00 (0.00)	0.00 (0.01)	0.04 (0.01)	0.07 (0.05)	0.00 (0.00)	0.01 (0.06)	0.04 (0.06)	0.06 (0.07)	0.00 (0.00)	0.01 (0.04)	0.01 (0.05)	0.01 (0.05)
	$snr = 8 : 2$	Power	0.56 (0.24)	0.86 (0.11)	0.94 (0.14)	0.95 (0.13)	0.76 (0.23)	.93 (0.02)	1.00 (0.04)	1.00 (0.03)	1.00 (0.00)	1.00 (0.00)	1.00 (0.00)	1.00 (0.00)
		FDR	0.00 (0.01)	0.00 (0.01)	0.06 (0.05)	0.09 (0.07)	0.00 (0.00)	0.00 (0.02)	0.04 (0.03)	0.07 (0.07)	0.01 (0.05)	0.02 (0.06)	0.02 (0.06)	0.02 (0.06)
	$snr = 7 : 3$	Power	0.42 (0.21)	0.77 (0.13)	0.91 (0.16)	0.94 (0.12)	0.73 (0.26)	0.94 (0.12)	0.95 (0.15)	0.96 (0.14)	1.00 (0.00)	1.00 (0.00)	1.00 (0.00)	1.00 (0.00)
		FDR	0.00 (0.00)	0.00 (0.01)	0.02 (0.03)	0.06 (0.04)	0.01 (0.05)	0.04 (0.06)	0.05 (0.07)	0.05 (0.09)	0.00 (0.02)	0.02 (0.05)	0.02 (0.05)	0.02 (0.06)
$\rho = 0.95$	$snr = 9 : 1$	Power	0.81 (0.19)	0.95 (0.07)	0.98 (0.06)	0.98 (0.07)	0.99 (0.04)	0.99 (0.03)	1.00 (0.00)	1.00 (0.00)	1.00 (0.00)	1.00 (0.00)	1.00 (0.00)	1.00 (0.00)
		FDR	0.00 (0.01)	0.03 (0.06)	0.03 (0.04)	0.05 (0.03)	0.00 (0.00)	0.04 (0.07)	0.08 (0.09)	0.09 (0.13)	0.00 (0.01)	0.03 (0.05)	0.07 (0.11)	0.10 (0.14)
	$snr = 8 : 2$	Power	0.65 (0.29)	0.84 (0.16)	0.89 (0.17)	0.89 (0.12)	0.94 (0.07)	0.97 (0.04)	0.99 (0.07)	0.99 (0.07)	1.00 (0.00)	1.00 (0.00)	1.00 (0.00)	1.00 (0.00)
		FDR	0.00 (0.03)	0.01 (0.05)	0.04 (0.06)	0.05 (0.06)	0.01 (0.03)	0.04 (0.04)	0.07 (0.14)	0.11 (0.11)	0.01 (0.02)	0.05 (0.09)	0.06 (0.14)	0.09 (0.11)
	$snr = 7 : 3$	Power	0.47 (0.22)	0.64 (0.17)	0.75 (0.19)	0.87 (0.11)	0.82 (0.27)	0.95 (0.10)	0.98 (0.04)	0.98 (0.02)	0.95 (0.10)	0.96 (0.11)	0.97 (0.08)	0.97 (0.06)
		FDR	0.00 (0.00)	0.02 (0.04)	0.02 (0.04)	0.04 (0.09)	0.00 (0.01)	0.04 (0.05)	0.09 (0.03)	0.13 (0.09)	0.00 (0.02)	0.04 (0.05)	0.05 (0.08)	0.08 (0.07)

C Model implementation details and Sensitivity Analysis

In this section, we mention the implementation details of SciDNet that we consider for the simulation study and real data analysis. To select the size of the active set \hat{S}_n in the screening step, in consistence with [35], we set $|\hat{S}_n| = \lfloor \frac{2n}{\log(n)} \rfloor$ by selecting the predictors with the top $|\hat{S}_n|$ Henze–Zirkler test statistic \tilde{w}_k^* , where $[z]$ denotes the integer part of z . In all our simulation scenarios, we set $r=0.9$, the hyperparameter for intra-cluster correlation bound to further integrate highly correlated conditionally dependent clusters. In cleaning step, for LassoNet 100 dimensional one-hidden-layer feed-forward neural network has been used; more detailed model architecture can be found at appendix in [18]. For creating the compact neighbourhood in the cleaning step, each time we choose the value of κ utilizing the phase transition property mentioned in section 2.2 of main manuscript. The feature selection performance of the SciDNet is demonstrated by calculating the average power and cFDR along with their standard error observed in 50 Monte Carlo replications. Each data set is randomly divided into train, validation and test with a 70-10-20 split. To asses the prediction performance, the test Mean Square Error (MSE) before and after the variable selection has been shown as part of the simulation study. For the prediction model, a 40-dimensional two-hidden-layer feed-forward neural network with ReLU and linear activation function is considered with Adam as optimizer.

To access the error bar for the sensitivity analysis, we generate a typical data using the polynomial setup (section 3 in main manuscript) and rerun SciDNet 50 times on the same data and set $q = 0.1$ as FDR-control threshold. The mean and standard deviations from these 50 replications are following: **power** = 1.00 (0.00), **observed FDR** = 0.00 (0.00), **test error by LassoNet** = 0.348 (0.2447349), **test error by SciDNet+LassoNet** = 0.321 (0.246). From computational complexity, after the screening, the bootstraped LassoNet can be run in parallel loop and we conduct all the experiments in a high-performing computing facility with Intel(R) Xeon(R) Platinum 8260 CPU @ 2.40GHz and 4 Tesla V100S. The codes are available at an anonymous repository (<https://anonymous.4open.science/r/SciDNet-EBBB>).

D Important clusters of gene discovered by SciDNet

First we present the phase transition property in Riboflavin reproduction data through Figure ???. The bootstrap standard deviations of the rank of the important scores are plotted. In x-acis, the clusters are ordered according to their importance. Clearly one would see the phase transition in variability after first few important clusters.

Following Table A7 shows the 5 selected clusters of gene selected by SciDNet while controlling the estimated surrogate FDR at $q = 0.15$. Interestingly, [6] found the gene *YCIC_at* as an important causal gene for riboflavin production, which is discovered by SciDNet in the clusters.

Table A7: Selected clusters of genes by SciDNet applied in the riboflavin gene data example

Cluster No.	Genes selected
1	EPR_at, IOLD_at, KAPB_at, PROJ_at, RPLQ_at, UREA_at, YCGB_at, YCGM_at, YCGN_at, YCSN_at, YCGO_at, YCGT_at, YDBM_at, YHXA_at, YKZC_at, YOAB_at, YPJB_at, YUSX_at, YVFH_at
2	COMX_at, CSPC_at, HAG_at, MPR_at, YBDL_at, YDBM_at, YHCB_at, YJFB_at, YHFS_at, YOAB_at, YODF_at, YOAC_at, YONU_at, YOTL_at, YQKL_at, YQZH_at, YTEL_at, YUSV_at
3	HIT_at, KATX_at, LICH_at, NASA_at, OPUCB_at, PHRG_i_at, PHRK_at, ROCB_at, ROCR_at, SACB_at, SPOIIE_at, TMRB_at, YACN_at, YBBJ_at, YBGB_at, YCBF_at, YFKJ_at, YHCS_at, YHXA_at, YJBF_at, YLBA_at, YLOU_at, YPUI_at, YQGY_i_at, YUKE_at, YVYD_at, YXLJ_at, YXZF_at
4	APPA_at, BGLS_at, ccpB_at, MMR_at, SIGY_at, SOJ_at, TREA_at, YBGB_at, YDGF_at, YOPR_at, YQEB_at, YVCI_at, YVDR_at, YWBG_at, YWDE_at, YWFM_at, YXBB_at, YXIL_at, YXIO_at, YXIQ_at, YXJA_at, YXJN_at, YXLC_at, YXLD_at, YXLE_at, YXLF_at, YXLG_at, YXLJ_at, YXZF_at, YYBF_at
5	YCDH_at, YCDI_at, YCEA_at, YCIA_at, YCIB_at, YCIC_at, YDAR_at, YHZA_at, YRPE_at, YTGA_at, YTGB_at, YTGC_at, YTGD_at, YTIA_at, YVQH_at